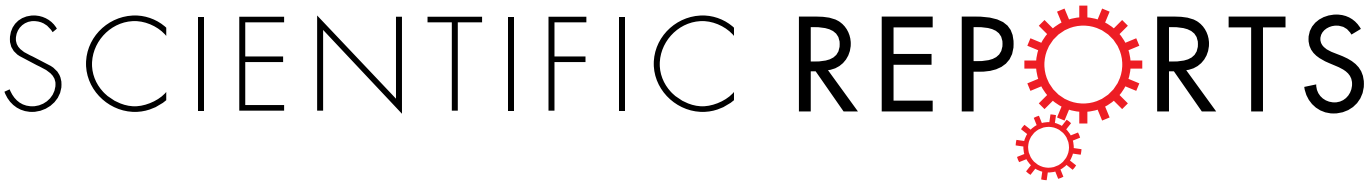

OPEN

Extremely large fractionation of Li isotopes in a chromitite-bearing mantle sequence

Received: 09 April 2015
Accepted: 15 February 2016
Published: 01 March 2016

Ben-Xun Su[1,2], Mei-Fu Zhou[2] & Paul T. Robinson[2]

We report Li isotopic compositions of olivine from the mantle sequence of the Luobusa ophiolite, southern Tibet. The olivine in the Luobusa ophiolite has Li concentrations from ~0.1 to 0.9 ppm and a broad range of δ^7Li (+14 to −20‰). An inverse correlation of Li concentration and δ^7Li in olivine from harzburgite suggests recent diffusive ingress of Li into the rock. Olivine from dunite enveloping podiform chromitites shows positive δ^7Li values higher than those of MORB, whereas olivine from the chromitite has negative δ^7Li values. Such variations are difficult to reconcile by diffusive fractionation and are thought to record the nature of the magma sources. Our results clearly indicate that the Luobusa chromitites formed from magmas with light Li isotopic compositions and that the dunites are products of melt-rock interaction. The isotopically light magmas originated by partial melting of a subducted slab after high degrees of dehydration and then penetrated the overlying mantle wedge. This study provides evidence for Li isotope heterogeneity in the mantle that resulted from subduction of a recycled oceanic component.

Recycling of oceanic lithosphere, mantle convection and crust-mantle interaction are processes that can produce isotopically heterogeneous mantle. Mantle heterogeneity induced by subduction is well constrained by the Li isotope system, which is sensitive to dehydration and metamorphism. ^{7}Li can be released preferentially from subducted slabs resulting in isotopically heavy mantle wedges and light residues[1–3]. Release of Li from the slabs to the mantle wedge is believed to be spatially variable both in amount and isotopic composition[1,4]. Heavy Li isotope signatures in OIBs (oceanic island basalts) appear to provide a geochemical tool for identifying recycled inputs into OIB sources[1,5–8]. However, partial melting residues enriched in isotopically light Li have only rarely been reported, but are important for understanding the fate of subducted slabs and the geochemical behavior of Li isotopes.

Light Li isotopic signals have been reported in a few abyssal peridotites and ophiolitic rocks[3,9,10]. Mantle sequences of ophiolites, particularly those with podiform chromitite deposits, were probably formed originally at mid-ocean ridges and then modified by melt-mantle interaction in suprasubduction zone environments[11–13]. The Luobusa ophiolite in southern Tibet has well-preserved mantle peridotites and podiform chromitites. Most of the podiform chromitites are enclosed in dunite envelopes, which clearly originated by interaction between peridotites and melts[12,13]. However, neither the nature nor the origin of the melts has been well constrained. Given that Li isotopes are important for tracing subduction-related processes[2,14–16] and melt-peridotite interaction[17–22], a ~20-cm-wide reaction zone in the Luobusa peridotite was selected for a detailed Li isotopic study to understand the extent of mantle heterogeneity at a sample scale. *In situ* Li isotopic analyses for olivine from this well-preserved reaction zone revealed dramatic changes of Li isotopic composition across the zone.

Geological background and petrography. The Tibetan Plateau was formed by the northward accretion of several terranes, separated by sutures, namely from south to north, The Yarlung-Zangbo, Bangong-Nujiang and Kohoxili suture zones. The Cretaceous Luobusa ophiolite lies in the eastern Yarlung Zangbo Suture Zone, about 200 km east-southeast of Lhasa. It contains both mantle and crustal rocks and hosts the largest chromite deposit in China[12,23,24]. The mantle sequence is composed of harzburgite, dunite and podiform chromitite. The harzburgites in this ophiolite are relatively refractory; all of the silicate minerals have high Mg#s [100 × Mg/(Mg + Fe)]

[1]State Key Laboratory of Lithospheric Evolution, Institute of Geology and Geophysics, Chinese Academy of Sciences, P.O. Box 9825, Beijing 10029, China. [2]Department of Earth Sciences, the University of Hong Kong, Pokfulam Road, Hong Kong, China. Correspondence and requests for materials should be addressed to B.-X.S. (email: subenxun@mail.igcas.ac.cn) or M.F.Z. (email: mfzhou@hku.hk)

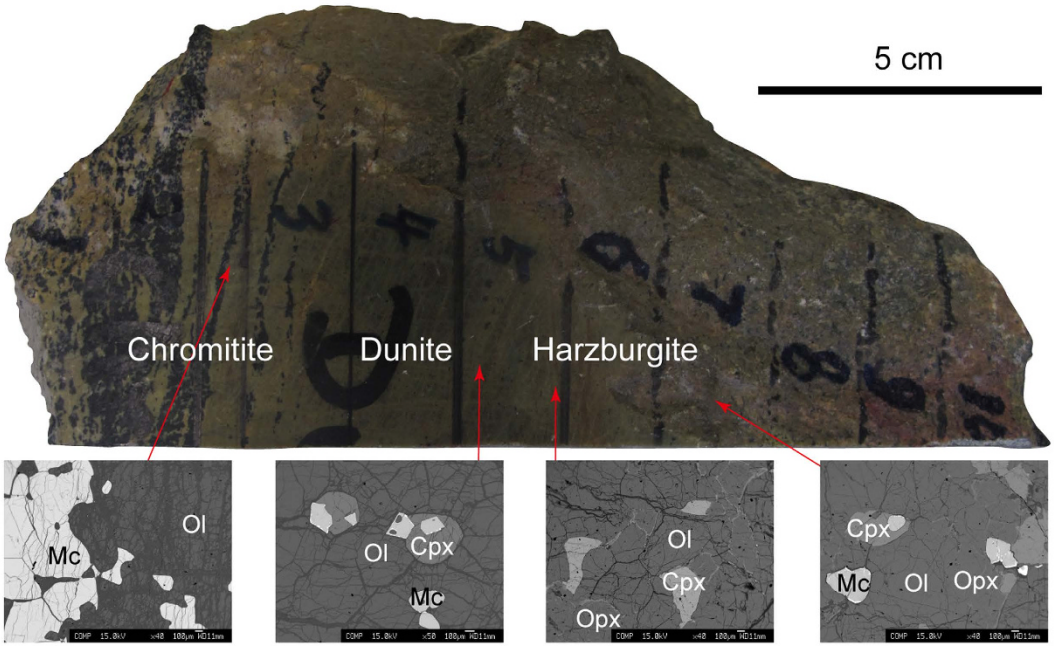

Figure 1. Photograph and back-scattered images of the sample consisting of harzburgite, dunite and chromitite of the Luobusa ophiolite, southern Tibet. Cpx, clinopyroxene; Mc, magnesiochromite; Ol, olivine; Opx, orthopyroxene.

of 92 to 96 and the magnesiochromite has variable Cr#s [100 × Cr/(Cr + Al)] from 30 to 76. The harzburgites also have very low bulk REE concentrations, with HREE ranging from 0.1 to 0.8 × chondrite, MREE from 0.05 to 0.2 × chondrite and LREE from 0.01 to 1.0 × chondrite, although many samples contain 2–3 modal% clinopyroxene[23]. Samples for this study were taken from a 20-cm-wide zone extending from a chromitite band through dunite to harzburgite (Fig. 1). The host harzburgite consists of ~70–75 modal% olivine (Fo_{92}), ~20–25% orthopyroxene (Mg# = 92), ~3% clinopyroxene (Mg# = 94) and 1–2% magnesiochromite (Mg# = 70; Cr# = 30). In contrast, the chromitite band consists of 10–50% high-Mg olivine (Fo_{95-96}) and 50–95% high-Cr magnesiochromite (Mg# = 57–62; Cr# = 74–76). Olivine is mostly interstitial to the magnesiochromite grains. As seen in Fig. 2, there are regular and systematic variations between the harzburgite and chromitite in mineral abundance and composition. Moving from the harzburgite to the chromitite, the abundance of pyroxene decreases (reaching zero in the dunite), whilst that of olivine increases (Fig. 1; ref. 23). All the silicate minerals show increases in Mg#, with olivine reaching a composition of Fo_{95} at the dunite-chromitite boundary (Fig. 2a). Although the abundance of magnesiochromite remains relatively constant in the harzburgite-chromitite transition zone, its Cr# increases to about 74 at the dunite-chromitite contact, which is relatively sharp (Fig. 2b). The lithologic and chemical characteristics of the studied samples (Figs 1 and 2) are identical to the reported data on harzburgite, dunite and chromitite of the Luobusa ophiolite[12,13,23,24], indicating that the samples are representative of the mantle sequence as a whole.

Lithium isotopic compositions of olivine. All of the olivine grains analyzed in this study, regardless of their host lithology, have low Li contents (~0.1 to 0.9 ppm). Olivine in the harzburgite generally has lower concentrations (0.13 to 0.35 ppm) than olivine in the dunite (0.30 to 0.60 ppm), however the concentration in the dunite drops markedly to 0.22 ppm at the contact with the chromitite band (Table S1; Fig. 2c). The δ^7Li values of olivine decrease from +13.6‰ in the Cpx-bearing harzburgite to +2.9‰ in the Cpx-poor harzburgite, and then increase again immediately adjacent to the dunite, only to drop steeply adjacent to the dunite-chromitite contact (Table S1; Fig. 2c). Olivine within the chromitite has variable Li abundances (0.20 to 0.90 ppm) and extreme isotopic heterogeneity, ranging from very light (-20‰) to MORB values (+7‰) (Fig. 2c). These olivine grains have δ^7Li values lower than those in the dunite zone and in the interlayered dunite within the chromitite. These variations correlate with variations in the Mg#s and FeO contents of both olivine and magnesiochromite (Figs 2 and 3).

Discussion

Primary features of Li isotopes. Because sediment pore water has variable and overall high δ^7Li values (0.0 to +46‰), fluid-rock interaction involving these media should enrich heavy Li isotope signatures of the rocks (Fig. 4a,b; refs 14, 25–30). Thus, this medium cannot account for the extremely low δ^7Li values of olivine in the Luobusa chromitite. Serpentinization removes Li, preferentially ^{6}Li, from the mineral grains to form Li-rich serpentine with low δ^7Li [26,31]. Thus, the involvement of serpentine from intergranular spaces and microcracks could potentially produce analyses with increased Li concentration but with decreased δ^7Li[9,31], unlike the decrease in Li concentration observed in the magnesiochromite bands, where microcracks are relatively well developed (Figs 1 and 2). High-temperature equilibrium fractionation of Li isotopes between melt and mantle peridotite is minor (<0.5‰) and produces covariations of δ^7Li and Li abundance[32,33], which are inconsistent with our results.

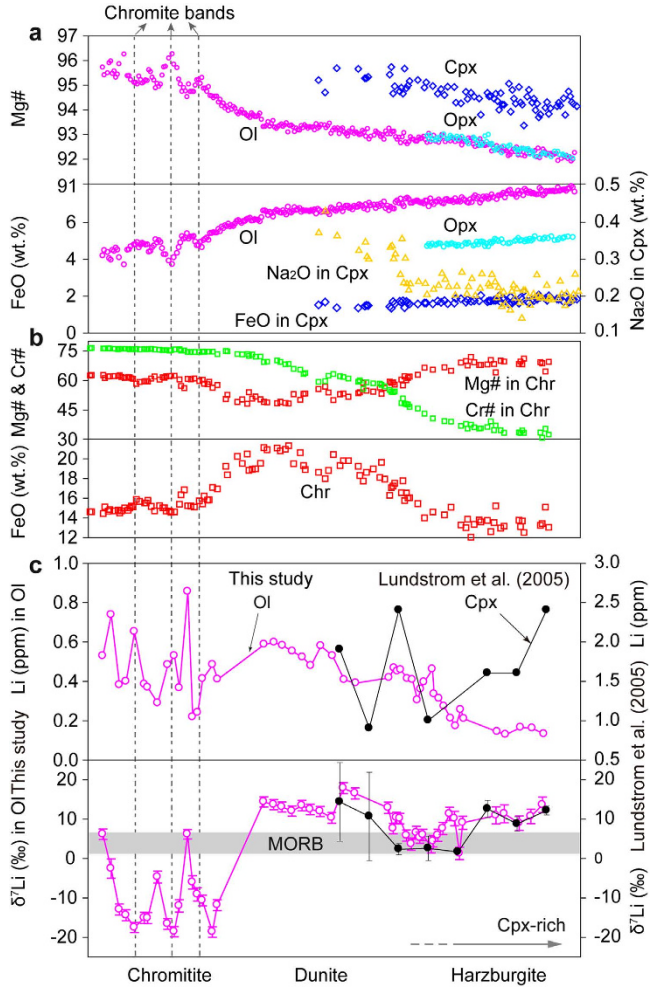

Figure 2. Chemical variations of minerals from harzburgite through dunite to chromitite. (**a**) Mg#, FeO and Na_2O contents of silicate minerals; (**b**) Mg#, Cr# and FeO contents of magnesiochromite; (**c**) Li isotopic and elemental variations of olivine. A compositional profile of clinopyroxene in lherzolite-harzburgite-dunite transect from the Trinity ophiolite[9] is also plotted for comparison.

Kinetic processes represent another possible means of altering Li isotopes. Diffusion-driven fractionation of Li isotopes generally assumes ingress of Li from an external source into rocks or minerals, such as diffusion of Li from Li-rich pegmatite into country rocks[34], or from olivine into coexisting clinopyroxene during cooling of peridotites[32,35]. In the case of Li diffusion from melts to wall-rock peridotites[9], the melts become progressively depleted in ^6Li because its diffusion rate is more rapid than ^7Li[31], leading to high-δ^7Li melts and low-δ^7Li wall-rock peridotites. This mechanism could potentially account for the observed decreases of δ^7Li with increasing Li abundance in olivine from the Luobusa harzburgite and clinopyroxene from the Trinity harzburgite[9] (Fig. 2c), suggesting diffusive ingress of Li into the harzburgite. However, such model does not adequately explain the observed isotopically light olivine with low Li abundance in the chromitite band and the ^7Li-rich olivine and high Li abundance of olivine in the dunite (Figs 2c and 3b). Studies by Dohmen *et al.*[36] and Ritcher *et al.*[37] revealed a complex diffusion behavior of Li and they accordingly proposed a coupled fast and slow diffusion mechanism. The fast mechanism of Li diffusion is unlikely to be dominant in most natural systems; under slow diffusion, the Li diffusion rate is about an order of magnitude faster than diffusion of Fe, Mg and many other divalent cations in olivine. Therefore, diffusion rate and cation exchange are relevant to the element content in the minerals. The overall decreasing FeO content and increasing Mg# in minerals, which show no correlations with Li variations in olivine in the harzburgite-dunite-chromitite profile (Fig. 2), could not have resulted solely from diffusion.

Thermal gradients can also fractionate Li isotopes resulting in ^7Li enrichment at the low-temperature end[38]. The harzburgite, occurring as wall rock of dunite in the Luobusa ophiolite[12,23], should have had a lower temperature than the melts from which the dunite formed. The contact between Cpx-poor harzburgite and dunite, however, has low δ^7Li signatures (Fig. 2c), contrary to what would be expected from thermal isotope fractionation.

Therefore, we conclude that the olivine in the Luobusa chromitite preserves primary Li abundances and isotopic compositions. Given that the mineral assemblage in the chromitite band consists only of olivine + magnesiochromite, and that the magnesiochromite structurally contains minor or no Li, we assume that the Li contents

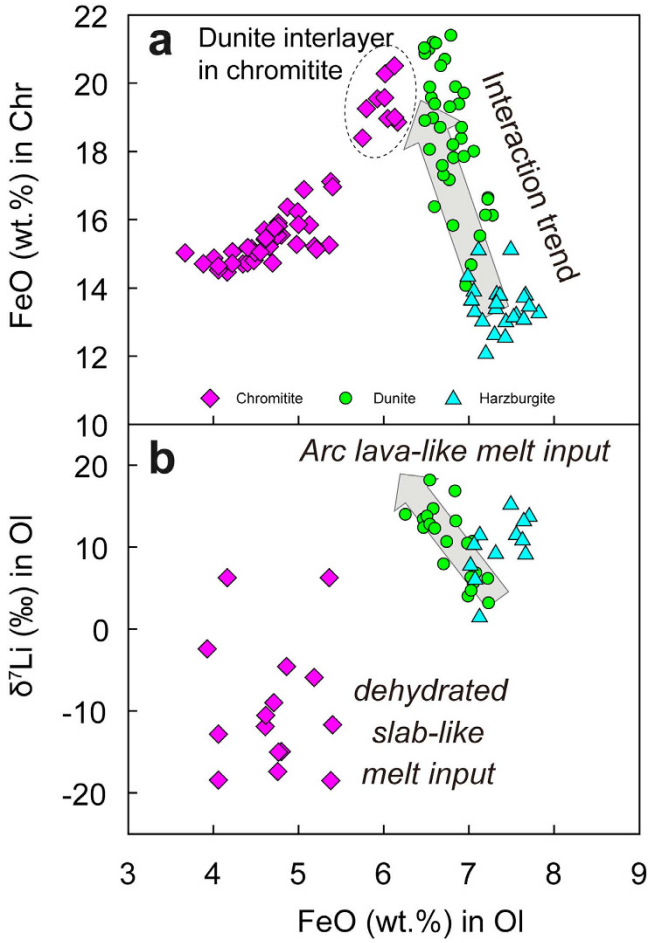

Figure 3. Diagrams of (**a**) FeO in olivine vs. FeO in magnesiochromite and (**b**) FeO in olivine vs. δ^7Li in olivine showing interaction trend from harzburgite to dunite and Li isotopic variations in the formation of dunite and chromitite.

and isotopic values in olivine of the Luobusa dunite and chromitite are representative of the whole rock samples and thus that the observed Li isotope heterogeneity in these samples reflects their mantle sources.

Constraints on the formation of dunite. Compositional changes of Li isotopes in olivine across the reaction zone are compatible with changes in FeO contents in the olivine and magnesiochromite (Figs 2 and 3) and Na_2O contents in the clinopyroxene (Fig. 2a). Similarly, there are also gradual changes in the whole-rock compositions, i.e. increasing LREE and IPGE and decreasing HREE and PPGE away from the harzburgite, accompanied by abrupt changes at the harzburgite-chromitite contact[23]. Similar Li isotopic variations in clinopyroxene were also reported along a lherzolite-harzburgite-dunite profile from the Trinity ophiolite, USA (Fig. 2c; ref. 9). This pattern is consistent with a reaction process whereby Li isotopes are fractionated during diffusion from melts in conduits to the surrounding peridotites. Such a reaction considerably raises the Li isotope ratios but has little influence on the absolute or relative abundances of the element in olivine and clinopyroxene (Figs 2b and 5; ref. 9). Bulk rock and mineral separates of ophiolitic peridotites and abyssal peridotites have low Li concentrations of <3 ppm, less than MORBs and OIBs (Fig. 4b), which can be attributed to melt extraction prior to peridotite-melt interaction. Therefore, Li isotopic variations in the harzburgite require a combined process of melt extraction and diffusion, which should also be responsible for the petrologic observation that clinopyroxene extends much farther toward the chromitite than orthopyroxene, because of the preferential dissolution of clinopyroxene during melting and preferential formation of clinopyroxene during metasomatism (Fig. 2a). The elevated δ^7Li values with an average of 10.1‰ in the dunite indicate that the heavy Li isotope signature was generated from a melt with a Li isotope composition falling in the range of arc lavas (δ^7Li $= -8.4$ to 11.4‰) (Fig. 4a). In the chromitite from the Luobusa ophiolite, olivine crystals in the interlayered dunite bands have the highest δ^7Li (Fig. 2c) and probably co-crystallized with those in the dunite, but they were subsequently modified by melts with light Li isotope signatures from which the magnesiochromite crystallized. Furthermore, the contrasting features of Li elemental and isotopic values in olivine from the chromitite suggest that its origin was different from that of the dunite.

Linking light δ^7Li of olivine in chromitite with a dehydrated slab. Rocks formed by prograde metamorphism undergo variable degrees of dehydration and generally display decreasing trends in δ^7Li values and

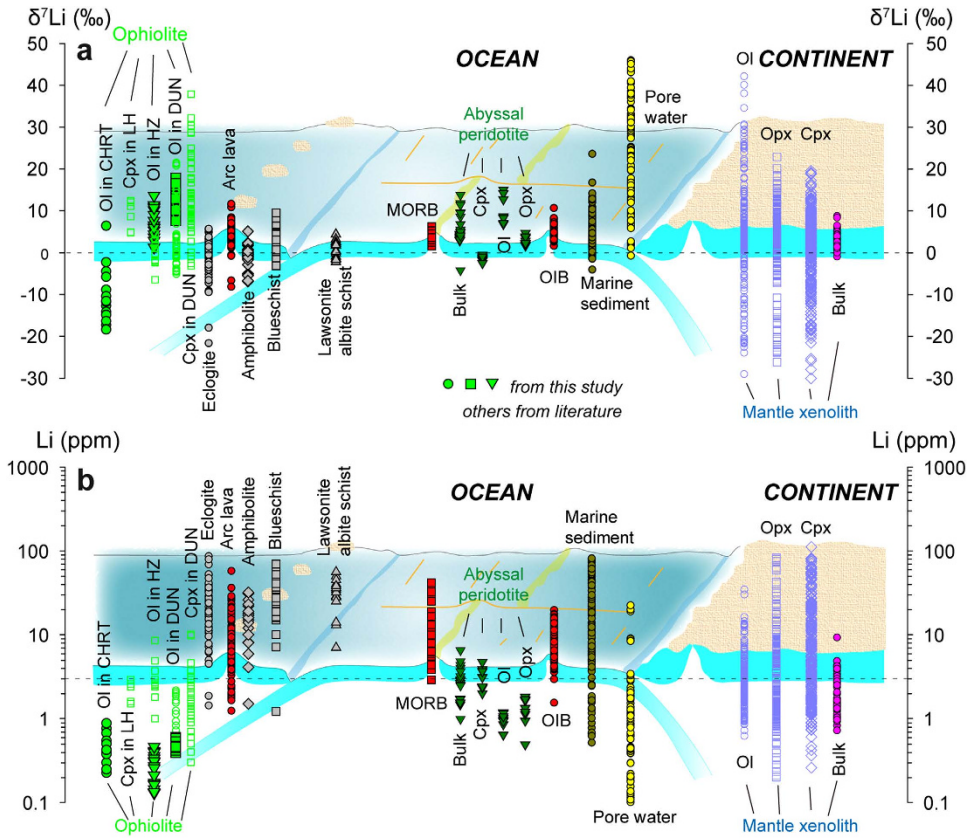

Figure 4. Li isotopic (**a**) and elemental (**b**) compositions of the main hosts and mineral separates in oceanic and continental settings. CHRT, chromitite; DUN, dunite; HZ, harzburgite; LZ, lherzolite. Marine sediment, refs 25, 26, 44 and 60; Pore water, ref. 25, 27 and 28; Arc lava, refs 1, 42–46 and 61; Abyssal peridotite, refs 3 and 10; Ophiolite, unfilled symbols from ref. 9 and filled symbols from this study; MORB, refs 6, 49 and 51; OIB, refs 7, 44, 50 and 52; Lawsonite albite schist, refs 39–41; Blueschist, refs 15, 39 and 40; Amphibolite, ref. 39; Eclogite, refs 2, 15 and 41; Bulk of peridotite xenolith, refs 18, 19, 32, 53–57; Olivine, orthopyroxene and clinopyroxene of peridotite xenoliths, refs 4, 21 and 22 and references therein.

Li abundances (Fig. 4), in the following order; lawsonite/albite schists (average Li = 30.8 ppm; δ^7Li = 0.93‰), blueschists (average Li = 28.6 ppm; δ^7Li = 2.36‰), amphibolites (average Li = 15.7 ppm; δ^7Li = −0.89‰) and eclogites (average Li = 22.6 ppm; δ^7Li = −1.49‰). On one hand, the Li isotopic variations in these metamorphic rocks are in very good agreement with the geochemical behavior of Li isotopes in subducted slabs during dehydration. That is, isotopically heavy Li is released into the mantle wedge in subduction zones, whereas the isotopically light component is subducted into the deeper mantle (Fig. 4; ref. 2). On the other hand, high Li concentrations in these metamorphic rocks are incompatible with expected Li behavior during dehydration because the process is expected to cause significant removal of Li from the rocks due to its moderately incompatible and fluid-affinity nature. Elevated Li concentrations and isotopic values in some of these rocks have been interpreted as resulting from Li addition from an aqueous fluid during exhumation and/or retrograde processes, because the rocks are presumed to have originally contained much lower Li concentrations and δ^7Li values under mantle conditions[2,15,39–41]. The heavy Li isotope released from the slabs probably contributes to the composition of arc lavas, whereas the isotopically light Li slab residues are subducted deep into the mantle[1,29,42–46], where they may form distinct reservoirs[2,4]. Light Li isotope melts have been observed in highly metasomatized mantle xenoliths that may have been derived from such reservoirs[4,21,22].

It is believed that the chromitites in Luobusa were precipitated from hydrous, high-Mg magmas undergoing differentiation (Fig. 3; refs 12 and 47). If the differentiation of the mafic magma was not accompanied by Li isotope fractionation[48], the large Li isotopic variation in olivine from the chromitites cannot be explained by this process. The low δ^7Li values, with an average of −10.2‰, and the low Li concentrations in olivine from the Luobusa chromitites (Figs 3, 4 and 5) are incompatible with dehydrated fluids from a subducted slab or an asthenospheric magma (e.g., MORB) but are most likely related to melting of a dehydrated slab[1,42–46]. The tearing and breakoff of the subducted slab, possibly along the transitional contact between amphibolites and eclogites, and subsequent asthenospheric upwelling probably caused partial melting of the dehydrated slab[13].

Different degrees of mixing between asthenospheric melts and slab melts can explain the large variations in Li concentrations and δ^7Li values. The involvement of a dehydrated slab should result in production of siliceous and oxidized melts that rapidly trigger magnesiochromite crystallization[12,13]. Magnesiochromite grains are suspended

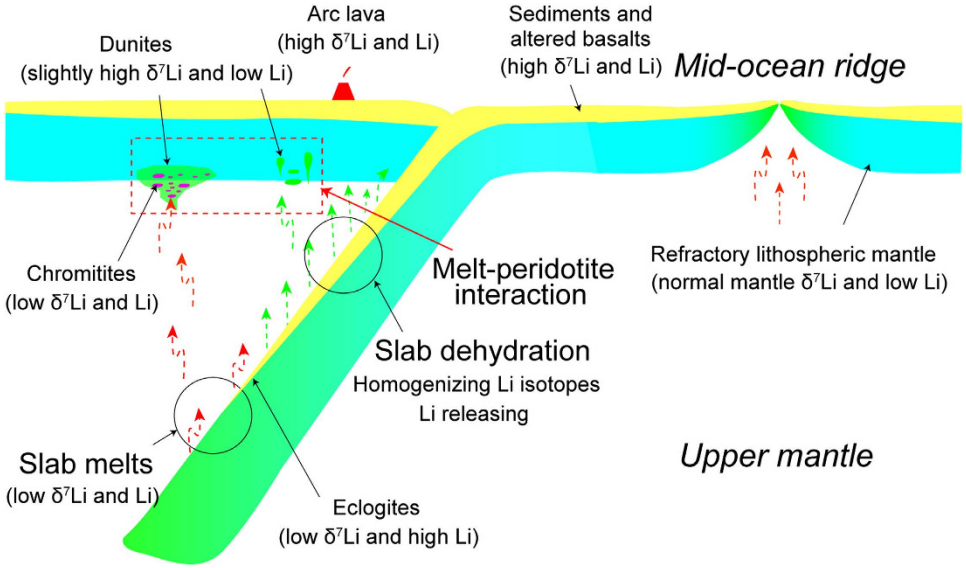

Figure 5. A cartoon showing variations of Li and its isotopes and formation of dunite and chromitite in an intra-oceanic subduction zone. The δ^7Li values and Li concentrations are relative to normal mantle values of δ^7Li = +2 to +6‰ and Li = 1 to 2 ppm (refs [6,22,49]). See exact ranges in Fig. 4. Although the formation of dunite and chromitite is treated as two processes in this model, we suggest that both are formed in a single, continuous process.

in upward-moving melts as they migrate through the overlying mantle wedge. Such melts eventually deposit magnesiochromite in magma conduits in the uppermost mantle. The formation of dunite and chromitite should be a continuous, linked process to account for the close affinity of dunite and chromitite in most ophiolites[13].

Implications for heterogeneous Li isotopes in the mantle. Studies of MORB lavas have revealed that they are derived from a relatively depleted mantle reservoir with a Li isotopic composition of δ^7Li = +1.6 to +6.2‰ (Fig. 4a; refs 6 and 49). Large-scale heterogeneity of the mantle has been documented in OIB lavas (+1.4 to +10.4‰; Fig. 4a; refs 7, 50–52) and mantle xenoliths (−1 to +10‰; refs 18, 19, 32, 53–57). Compared to MORB and OIB lavas, fresh oceanic peridotites (bulk: δ^7Li = −4.2 to + 13.8‰; refs 3 and 10) and those from ophiolites (i.e. olivine in dunite and chromitite) have much larger Li isotopic variations (δ^7Li = −18.6 to +21.3‰) (ref. 9 and this study). Likewise, mantle xenoliths display ~60‰ δ^7Li variation among their constituent minerals (Fig. 4a), although much of the variability is poorly constrained, indicating highly variable Li isotopes in xenoliths. These data indicate that the lithospheric mantle is more heterogeneous in Li isotopes and preserves more compositional signatures from slab melts than the asthenospheric mantle, and that Li isotopes are not necessarily equilibrated at mantle temperatures as previously expected[32,35].

In a global perspective, oceanic crust recycled into the mantle via subduction could be partly returned to the Earth's surface by means of dehydration, magmatism and exhumation. However, subducted slabs and their stagnant fragments in the mantle are far less voluminous than the oceanic crust that once existed[58]. Most of the fragments were probably successively involved in melt-peridotite interaction in oceanic subduction zones to facilitate the large volumes of melt needed for the modification of the oceanic mantle and occasional formation of podiform chromitite deposits[13]. Because dehydrated slabs would be depleted in Li due to dehydration, their light isotopic signature might be easily overprinted upon reaction with peridotites.

Conclusions

The Luobusa ophiolite preserves Li isotopic variations produced both during formation at mid-ocean ridges and by subsequent modification in a suprasubduction zone setting. Olivine from the harzburgite shows negative co-variation between Li concentrations and δ^7Li values due to diffusive ingress of Li from the melts. The Li isotopic features of the dunite are comparable to arc-like melts. The melts from which the magnesiochromite crystallized are inferred to have been depleted in Li content and enriched in ^{6}Li relative to ^{7}Li, thus producing values inferred for highly dehydrated slabs. These two types of melts continuously and progressively reacted with the oceanic lithospheric mantle, resulting in the formation of dunite and chromitite, and accounting for the observed Li isotope heterogeneity.

Methods

Major element analysis. Major element compositions of minerals were determined by wavelength dispersive spectrometry using JEOL JXA8100 electron probe microanalyzer (EPMA) at the Institute of Geology and Geophysics, Chinese Academy of Sciences (IGGCAS), Beijing, China. The EPMA analyses were carried out at an accelerating voltage of 15 kV and 10 nA beam current, 5 μm beam spot and 10–30 s counting time on peak.

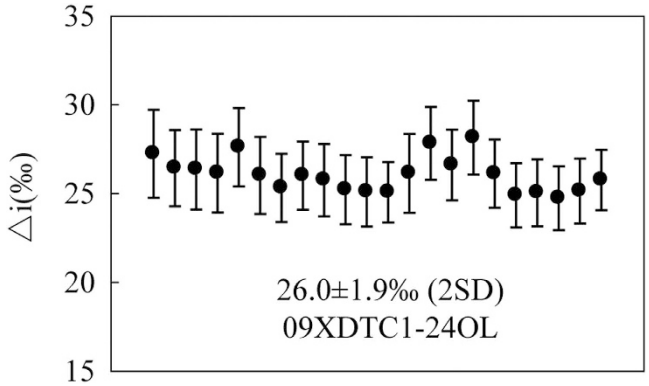

Figure 6. Standard Li isotopic variation throughout the analyses with 2σ error bars.

Natural and synthetic minerals were used for standard calibration. A program based on the ZAF procedure was used for matrix corrections. Typical analytical uncertainty for all of the elements analyzed is better than 1.5%.

Li isotope analysis. *In situ* Li isotope measurements of olivine on thin sections were performed on Cameca IMS-1280 SIMS at IGGCAS. The O^- primary ion beam was accelerated at 13 kV, with an intensity of about 15 to 30 nA. The elliptical spot was approximately 20 × 30 μm in size. Positive secondary ions were measured on an ion multiplier in pulse counting mode, with a mass resolution (M/DM) of 1500 and an energy slit open at 40 eV without any energy offset. A 180-second pre-sputtering without raster was applied before analysis. The secondary ion beam position in the contrast aperture, as well as the magnetic field and the energy offset, was automatically centred before each measurement. Thirty cycles were measured with counting times of 12, 4 and 4 seconds for ^{6}Li, background at the 6.5 mass, and ^{7}Li, respectively. Olivine sample 09XDTC1-24OL with Fo of 94.2 was used as standard[59] and its similar composition to the analyzed olivine eliminates any possible contribution of matrix to the observed data. The measured δ^7Li values are given as $\delta^7\text{Li} = ([(^7\text{Li}/^6\text{Li})_{\text{sample}}/(^7\text{Li}/^6\text{Li})_{\text{L-SVEC}} - 1] \times 1000)$ relative to units of the standard NIST SRM 8545 (L-SVEC). The instrumental mass fractionation is expressed in $\delta^7\text{Li} = \delta^7\text{Li}_{\text{SIMS}} - \delta^7\text{Li}_{\text{MC-ICPMS}}$. Twenty two analyses on the standard in the study yielded homogeneous Li isotopic composition with $\Delta\text{i} = 26.0 \pm 1.9‰$ (2SD) (Fig. 6). Matrix effect, of which δ^7Li increased by 1.0‰ for each mole percent decrease in forsterite component of olivine[59], was considered for calibration. The external 2σ errors of the isotope compositions for both the standards and the samples are less than 2.5‰.

References

1. Chan, L. H., Leeman, W. P. & You, C. F. Lithium isotopic composition of Central American volcanic arc lavas: implications for modification of subarc mantle by slab-derived fluids: correction. *Chem. Geol.* **182,** 293–300 (2002).
2. Zack, T., Tomascak, P. B., Rudnick, R. L., Dalpe, C. & McDonough, W. F. Extremely light Li in orogenic eclogites: the role of isotope fractionation during dehydration in subducted oceanic crust. *Earth Planet. Sci. Lett.* **208,** 279–290 (2003).
3. Brooker, R. A., James, R. H. & Blundy, J. D. Trace elements and Li isotope systematics in Zabargad peridotites: evidence of ancient subduction processes in the Red Sea mantle. *Chem. Geol.* **212,** 179–204 (2004).
4. Tang, Y. J. *et al.* Abnormal lithium isotope composition from the ancient lithospheric mantle beneath the North China Craton. *Sci. Rep.* **4,** 4274 (2014).
5. Nishio, Y. *et al.* Lithium isotopic systematics of the mantle-derived ultramafic xenoliths: implications for EM1 origin. *Earth Planet. Sci. Lett.* **217,** 245–261 (2004).
6. Tomascak, P. B., Langmuir, C. H., le Roux, P. & Shirey, S. B. Lithium isotopes in global mid-ocean ridge basalts. *Geochim. Cosmochim. Acta* **72,** 1626–1637 (2008).
7. Vlastelic, I., Koga, K., Chauvel, C., Jacques, G. & Telouk, P. Survival of lithium isotopic heterogeneities in the mantle supported by HIMU-lavas from Rurutu Island, Austral Chain. *Earth Planet. Sci. Lett.* **286,** 456–466 (2009).
8. Magna, T. *et al.* Lithium in tektites and impact glasses: Implications for sources, histories and large impacts. *Geochim. Cosmochim. Acta* **75,** 2137–2158 (2011).
9. Lundstrom, C. C., Chaussidon, M., Hsui, A. T., Kelemen, P. & Zimmerman, M. Observations of Li isotopic variations in the Trinity Ophiolite: Evidence for isotopic fractionation by diffusion during mantle melting. *Geochim. Cosmochim. Acta* **69,** 735–751 (2005).
10. Gao, Y., Snow, J. E., Casey, J. F. & Yu, J. Cooling-induced fractionation of mantle Li isotopes from the ultraslow-spreading Gakkel Ridge. *Earth Planet. Sci. Lett.* **301,** 231–240 (2011).
11. Kelemen, P. B., Dick, H. J. B. & Quick, J. E. Formation of harzburgite by pervasive melt/rock reaction in the upper mantle. *Nature* **358,** 635–641 (1992).
12. Zhou, M. F., Robinson, P. T., Malpas, J. & Li, Z. Podiform chromites in the Luobusa Ophiolite (southern Tibet): implications for melt-rock interaction and chromite segregation in the upper mantle. *J. Petrol.* **37,** 3–21 (1996).
13. Zhou, M. F. *et al.* Compositions of chromite, associated minerals, and parental magmas of podiform chromite deposits: The role of slab contamination of asthenospheric melts in suprasubduction zone environments. *Gondwana Res.* **25,** 1429–1451 (2014).
14. Elliott, T., Jeffcoate, A. & Bouman, C. The terrestrial Li isotope cycle: light-weight constraints on mantle convection. *Earth Planet. Sci. Lett.* **220,** 231–245 (2004).
15. Marschall, H. R., Pogge von Strandmann, P. A. E., Seitz, H. M., Elliott, T. & Niu, Y. L. The lithium isotopic composition of orogenic eclogites and deep subducted slabs. *Earth Planet. Sci. Lett.* **262,** 563–580 (2007).
16. Agostini, S., Ryan, J. G., Tonarini, S. & Innocenti, F. Drying and dying of a subducted slab: Coupled Li and B isotope variations in Western Anatolia Cenozoic volcanism. *Earth Planet. Sci. Lett.* **272,** 139–147 (2008).
17. Seitz, H. M. & Woodland, A. B. The distribution of lithium in peridotitic and pyroxenitic mantle lithologies—an indicator of magmatic and metasomatic processes. *Chem. Geol.* **166,** 47–64 (2000).

18. Tang, Y. J. *et al.* Lithium isotopic systematics of peridotite xenoliths from Hannuoba, North China Craton: Implications for melt-rock interaction in the considerably thinned lithospheric mantle. *Geochim. Cosmochim. Acta* **71,** 4327–4341 (2007).
19. Magna, T., Ionov, D. A., Oberli, F. & Wiechert, U. Links between mantle metasomatism and lithium isotopes: Evidence from glass-bearing and cryptically metasomatized xenoliths from Mongolia. *Earth Planet. Sci. Lett.* **276,** 214–222 (2008).
20. Zhang, H. F., Deloule, E., Tang, Y. J. & Ying, J. F. Melt/rock interaction in remains of refertilized Archean lithospheric mantle in Jiaodong Peninsula, North China Craton: Li isotopic evidence. *Contrib. Mineral. Petrol.* **160,** 261–277 (2010).
21. Su, B. X. *et al.* Extremely high Li and low δ^7Li signatures in the lithospheric mantle. *Chem. Geol.* **292–293,** 149–157 (2012).
22. Su, B. X. *et al.* Distinguishing silicate and carbonatite mantle metasomatism by using lithium and its isotopes. *Chem. Geol.* **381,** 67–77 (2014).
23. Zhou, M. F., Robinson, P. T., Malpas, J., Edwards, S. & Qi, L. REE and PGE geochemical constraints on the formation of dunites in the Luobusa ophiolite, Southern Tibet. *J. Petrol.* **46,** 615–639 (2005).
24. Xiong, F. H. *et al.* Origin of podiform chromitite, a new model based on the Luobusa ophiolite, Tibet. *Gondwana Res.* **27,** 525–542 (2015).
25. Zhang, L., Chan, L. H. & Gieskes, J. M. Lithium isotope geochemistry of pore waters, Ocean Drilling Program Sites 918 and 919, Irminger Basin. *Geochim. Cosmochim. Acta* **62,** 2437–2450 (1998).
26. Chan, L. H., Alt, J. C. & Teagle, D. A. H. Lithium and lithium isotope profiles through the upper oceanic crust: a study of seawater-basalt exchange at ODP Sites 504B and 896A. *Earth Planet. Sci. Lett.* **201,** 187–201 (2002).
27. Pogge von Strandmann, P. A. E. *et al.* Lithium, magnesium and silicon isotope behaviour accompanying weathering in a basaltic soil and pore water profile in Iceland. *Earth Planet. Sci. Lett.* **339,** 11–23 (2012).
28. Scholz, F. *et al.* Lithium isotope geochemistry of marine pore waters–insights from cold seep fluids. *Geochim. Cosmochim. Acta* **74,** 3459–3475 (2010).
29. Harrison, L., Weis, D., Hanano, D. & Barnes, E. Lithium isotopic signature of Hawaiian basalts. *Hawaiian Volcanoes: From Source to Surface* 79–104 (2015).
30. Tang, M., Rudnick, R. L. & Chauvel, C. Sedimentary input to the source of Lesser Antilles lavas: a Li perspective. *Geochim. Cosmochim. Acta* **144,** 43–58 (2014).
31. Decitre, S. E. *et al.* Behavior of Li and its isotopes during serpentinization of oceanic peridotites. *Geochem. Geophys. Geosyst.* **3,** 10.1029/2001GC000178 (2002).
32. Jeffcoate, A. B. *et al.* Li isotope fractionation in peridotites and mafic melts. *Geochim. Cosmochim. Acta* **71,** 202–218 (2007).
33. Wagner, C. & Deloule, E. Behaviour of Li and its isotopes during metasomatism of French Massif Central lherzolites. *Geochim. Cosmochim. Acta* **71,** 4279–4296 (2007).
34. Teng, F. Z., McDonough, W. F., Rudnick, R. L. & Walker, R. J. Diffusion-driven extreme lithium isotopic fractionation in country rocks of the Tin Mountain pegmatite. *Earth Planet. Sci. Lett.* **243,** 701–710 (2006).
35. Parkinson, I. J., Hammond, S. J., James, R. H. & Rogers, N. W. High-temperature lithium isotope fractionation: Insights from lithium isotope diffusion in magmatic systems. *Earth Planet. Sci. Lett.* **257,** 609–621 (2007).
36. Dohmen, R., Kasemann, S. A., Coogan, L. & Chakraborty, S. Diffusion of Li in olivine. Part I: experimental observations and a multi species diffusion model. *Geochim. Cosmochim. Acta* **74,** 274–292 (2010).
37. Richter, F., Watson, B., Chaussidon, M., Mendybaev, R. & Ruscitto, D. Lithium isotope fractionation by diffusion in minerals. Part 1: Pyroxenes. *Geochim. Cosmochim. Acta* **126,** 352–370 (2014).
38. Richter, F. *et al.* Isotope fractionation of Li and K in silicate liquids by Soret diffusion. *Geochim. Cosmochim. Acta* **138,** 136–145 (2014).
39. Penniston-Dorland, S. C., Bebout, G. E., Pogge von Strandmann, P. A. E., Elliott, T. & Sorensen, S. S. Lithium and its isotopes as tracers of subduction zone fluids and metasomatic processes: Evidence from the Catalina Schist, California, USA. *Geochim. Cosmochim. Acta* **77,** 530–545 (2012).
40. Penniston-Dorland, S. C., Sorensen, S. S., Ash, R. D. & Khadke, S. V. Lithium isotopes as a tracer of fluids in a subduction zone mélange: Franciscan Complex, CA. *Earth Planet. Sci. Lett.* **292,** 181–190 (2010).
41. Simons, K. K. *et al.* Lithium isotopes in Guatemalan and Franciscan HP–LT rocks: Insights into the role of sediment-derived fluids during subduction. *Geochim. Cosmochim. Acta* **74,** 3621–3641 (2010).
42. Tomascak, P. B., Ryan, J. G. & Defant, M. J. Lithium isotope evidence for light element decoupling in the Panama subarc mantle. *Geology* **28,** 507–510 (2000).
43. Tomascak, P. B., Widom, E., Benton, L. D., Goldstein, S. L. & Ryan, J. G. The control of lithium budgets in island arcs. *Earth Planet. Sci. Lett.* **196,** 227–238 (2002).
44. Leeman, W. P., Tonarini, S., Chan, L. H. & Borg, L. E. Boron and lithium isotopic variations in a hot subduction zone–the southern Washington Cascades. *Chem. Geol.* **212,** 101–124 (2004).
45. Magna, T., Wiechert, U., Grove, T. L. & Halliday, A. N. Lithium isotope fractionation in the southern Cascadia subduction zone. *Earth Planet. Sci. Lett.* **250,** 428–443 (2006a).
46. Chan, L. H., Lassiter, J. C., Hauri, E. H., Hart, S. R. & Blusztajn, J. Lithium isotope systematics of lavas from the Cook-Austral Islands: Constraints on the origin of HIMU mantle. *Earth Planet. Sci. Lett.* **277,** 433–442 (2009).
47. Rollinson, H. & Adetunji, J. Mantle podiform chromitites do not form beneath mid-ocean ridges: A case study from the Moho transition zone of the Oman ophiolite. *Lithos* **177,** 314–327 (2013).
48. Tomascak, P. B., Tera, F., Helz, R. T. & Walker, R. J. The absence of lithium isotope fractionation during basalt differentiation: new measurements by multi-collector sector ICP-MS. *Geochim. Cosmochim. Acta* **63,** 907–910 (1999).
49. Elliott, T., Thomas, A., Jeffcoate, A. & Niu, Y. L. Lithium isotope evidence for subduction-enriched mantle in the source of midocean-ridge basalts. *Nature* **443,** 565–568 (2006).
50. Ryan, J. G. & Kyle, P. R. Lithium abundance and lithium isotope variations in mantle sources: insights from intraplate volcanic rocks from Ross Island and Marie Byrd Land (Antarctica) and other oceanic islands. *Chem. Geol.* **212,** 125–142 (2004).
51. Schuessler, J. A., Schoenberg, R. & Sigmarsson, O. Iron and lithium isotope systematics of the Hekla volcano, Iceland—Evidence for Fe isotope fractionation during magma differentiation. *Chem. Geol.* **258,** 78–91 (2009).
52. Krienitz, M. S. *et al.* Lithium isotope variations in ocean island basalts: Implications for the development of mantle heterogeneity. *J. Petrol.* **53,** 2333–2347 (2012).
53. Seitz, H. M., Brey, G. P., Lahaye, Y., Durali, S. & Weyer, S. Lithium isotopic signatures of peridotite xenoliths and isotopic fractionation at high temperature between olivine and pyroxenes. *Chem. Geol.* **212,** 163–177 (2004).
54. Magna, T., Wiechert, U. & Halliday, A. N. New constraints on the lithium isotope compositions of the Moon and terrestrial planets. *Earth Planet. Sci. Lett.* **243,** 336–353 (2006b).
55. Ionov, D. A. & Seitz, H. M. Lithium abundances and isotopic compositions in mantle xenoliths from subduction and intra-plate settings: mantle sources vs. eruption histories. *Earth Planet. Sci. Lett.* **266,** 316–331 (2008).
56. Aulbach, S. & Rudnick, R. L. Origins of non-equilibrium lithium isotope fractionation in xenolithic peridotite minerals: examples from Tanzania. *Chem. Geol.* **258,** 17–27 (2009).
57. Halama, R., Savov, I. P., Rudnick, R. L. & McDonough, W. F. Insights into Li and Li isotope cycling and sub-arc metasomatism from veined mantle xenoliths, Kamchatka. *Contrib. Mineral. Petrol.* **158,** 197–222 (2009).
58. Zhao, D. P. Global tomographic images of mantle plumes and subducting slabs: insight into deep Earth dynamics. *Physics Earth Planet. Interi.* **146,** 3–34 (2004).

59. Su, B. X. *et al.* Potential orthopyroxene, clinopyroxene and olivine reference materials for *in situ* lithium isotope determination. *Geostand. Geoanal. Res.* **39,** 357–369 (2015).
60. Chan, L. H., Leeman, W. P. & Plank, T. Lithium isotopic composition of marine sediments. *Geochem. Geophys. Geosyst.* **7,** doi: 10.1029/2005GC001202 (2006).
61. Kosler, J. *et al.* Combined Sr, Nd, Pb and Li isotope geochemistry of alkaline lavas from northern James Ross Island (Antarctic Peninsula) and implications for back-arc magma formation. *Chem. Geol.* **258,** 207–218 (2009).

Acknowledgements

We thank Qiu-Li Li, Guo-Qiang Tang and Yu Liu for assistance with the SIMS analyses, and Kwan-Nang Pang, Patrick Asamoah Sakyi and Yan-Jie Tang for polishing the paper. Constructive reviews from three anonymous reviewers are highly appreciated. This study was supported by the Strategic Priority Research Program (B) of the Chinese Academy of Sciences (Grant No. XDB03010203) and the National Natural Science Foundation of China (Grants 41173011 and 41473038).

Author Contributions

M.F.Z. and P.T.R. collected the samples. B.X.S. conducted the chemical analyses. B.X.S. and M.F.Z. wrote the main text. B.X.S., M.F.Z. and P.T.R. contributed equally to the intellectual growth of this paper.

Additional Information

Supplementary information accompanies this paper at http://www.nature.com/srep

Competing financial interests: The authors declare no competing financial interests.

How to cite this article: Su, B.-X. *et al.* Extremely large fractionation of Li isotopes in a chromitite-bearing mantle sequence. *Sci. Rep.* **6**, 22370; doi: 10.1038/srep22370 (2016).